Impact of Hybrid Energy Storage System (HESS) Topologies on Performance: Exploration for Hydropower Hybrids

Abhishek Banerjee
Idaho National Laboratory
Abhishek.Banerjee@inl.gov

S M Shafiul Alam
Idaho National Laboratory
SMShafiul.Alam@inl.gov

Thomas M Mosier
Idaho National Laboratory
Thomas.Mosier@inl.gov

Abstract

We investigate the technical performance of six HESS topologies integrated with run-of-river (ROR) hydropower to provide frequency support. We choose ROR hydropower because there are 23 GW of installed ROR hydropower in the U.S. and integrating these plants with energy storage could boost their contribution to grid services. We focus on HESSs composed of batteries and ultracapacitors because batteries are cost effective for storing energy but degrade more quickly as a function of cycling. In contrast, ultracapacitors can be cycled millions of times and are cost effective for quick injections of power. We find that active HESS topologies demonstrate the best overall improvement to grid frequency during a contingency while adhering to the power ramping limits of the HESS devices. Future work will investigate other services to identify if one HESS topology performs best for all services of interest or, more likely, different HESS topologies are best suited for specific services.

1. Introduction: Importance of Energy Storage and Hydropower

Energy storage technologies are rapidly evolving: energy density, ramping capability and longevity are increasing at the same time that costs have been reducing significantly [1]. This is leading to rapid scaling of energy storage deployment and consideration of integrating generation resources and energy storage systems. The value of integration is that the energy storage technology can perform actions that are either not economical for the generation resource (e.g. without the energy storage would lead to operating off the peak efficiency) [2] or would increase operations and maintenance costs [3]. Energy storage integration can also enable new capabilities for the generation resource, such as increasing ramping speed of the integrated system.

Hybrid energy storage systems (HESS) expand on this concept further by identifying complementary energy storage technologies that can be paired through physical integration and optimized through coordinated control to complement one another. An example of this is pairing batteries and ultracapacitors (UCAPs), which is widely being used in electric vehicles industries [4, 5, 6, 7]. The potential benefit of this HESS is that the batteries are more economically scalable with respect to total energy storage (i.e. MWh) but degrade over fewer cycles than UCAPs [1]. UCAPs can also respond extremely quickly and tolerate more diverse cycling conditions (e.g. rapid, deep cycling) better than batteries. Yet, only a single grid-scale application of such pair is known to exist for solar generation smoothing [8]. Therefore, there needs to have a service specific optimal design strategy that extends the financial and technical performance of the HESS through grid-scale integration of batteries and UCAPs.

The hybrid topology for energy storage systems determines controllability and limits or enables technical performance of the individual energy storage devices and their combined output. There is a spectrum of possible topologies, detailed further below, ranging from passive to full-active. In a passive topology, both the battery and UCAP are connected in parallel and operated with a common voltage, offering the cheapest configuration of hybrid system, in the absence of control and power electronic circuitries. Whereas, in a full-active topology, battery and UCAP are coupled via their dedicated DC-DC converters, offering the most stable, and the most flexible operation [9]. Additionally, there are several combinations in between that differ with respect to converter choice and placement.

The benefits of integrating a HESS with a generation resource will depend on the specific capabilities and performance requirements of that generation resource. Hydropower is one of very few types of renewable generation resource with physical inertia. Furthermore, it is less variable and more predictable than solar and wind energy [10]. Run-of- river (ROR) - one of the variants of hydropower constitutes 23 GW of installed

URI: https://hdl.handle.net/10125/70993
978-0-9981331-4-0

capacity in the U.S. [11]. As the electric grid needs shift more towards grid services and away from energy, this installed hydropower capacity would benefit from mechanisms to boost its contribution to the electric grid and integration with energy storage is one promising pathway to achieve this. For example, American Electric Power (AEP) has integrated batteries with two of their hydropower plants, the Buck and Byllesby ROR hydropower plants, to enhance their ability to provide an automatic generation control (AGC) dispatched frequency regulation in the PJM (Pennsylvania-New Jersey-Maryland) ancillary services market [12].

There are a wide range of ROR hydropower facilities that differ in terms of their turbine-generator technologies, capacity, and amount of flexibility. Some ROR hydropower plants are required to balance inflow and outflow on a daily basis, thus having some storage and corresponding flexibility, whereas other plants are strictly non-dispatchable and are therefore "must take" generation resources.

In this paper, we explore the impact of HESS topology on combined response of a non-dispatchable ROR hydropower plant and HESS to a grid event. We focus on the droop-control based *frequency response*, which is necessary to maintain the integrated system capable of providing any AGC dispatched regulation service as in [12]. The objective is to determine the differences in technical performance and identify specific HESS topologies that are better suited for this type of integration. Different events like loading changes, temporary fault scenarios were simulated to test the performance of the hybrids with respect to each scenario. The HESS modules were integrated to the ROR hydropower plant by a DC coupled network in the current injection framework. The hydropower generator is equipped with hydro-governor and exciter models that are tuned to optimal setting for providing adequate improvements in the frequency nadir. The contribution of this work is to motivate consideration of specific HESS topologies for pairing with ROR hydropower resources to maximize performance for specific objectives, such as responding to a load trip event.

The paper is further organized as: Sec. 2 defines the topologies assessed for creating HESS integration with ROR hydropower; Sec. 3 describes the simulation framework, including grid configuration and contingencies tested; Sec. 4 presents the simulation results; and Sec. 5 provides concluding remarks and future research directions.

2. Topologies for Creating HESS and Integrating with ROR Hydropower

The key energy storage focus here is on differences in topologies that may be used to integrate HESS with ROR hydropower systems to increase capabilities and performance of the integrated HESS and generation system. Each of the HESS topologies include a battery and UCAP. This section explains the energy storage topologies considered.

2.1. Passive HESS

The simplest method of combining two energy storage devices is a parallel connection which is also known as the "passive" configuration (Fig. 1). The passive HESS involves direct coupling of the battery and the UCAP without the use of any external interfacing converter and keeps the two storage devices at the same voltage level. The battery and the UCAP share the same terminal voltage that depends on the state-of-charge (SoC) and charge/discharge characteristic of the battery.

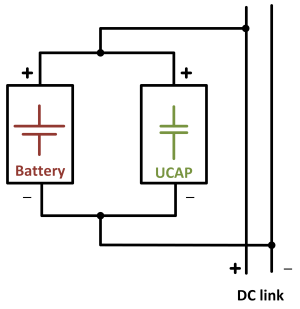

Figure 1. Passive HESS topology.

This is a direct connection where the HESS is coupled to the DC bus without using any DC-DC converters. This results in having no control over the active power flow through these storage devices. The current drawn from the battery and UCAP depends on their respective internal resistances [13]. Therefore, the transient power handling capability of the UCAP is under utilized. And, the ramp up (and down) power in response to a frequency nadir (zenith) is mainly provided by means of the battery. In addition, as the voltage variation of the battery terminal is small, the UCAP will not be operating at its full SoC range, which results in poor volumetric efficiency [14]. The advantages of passive HESS are the simplicity and low implementation cost because of the absence of power electronics and control circuits [15].

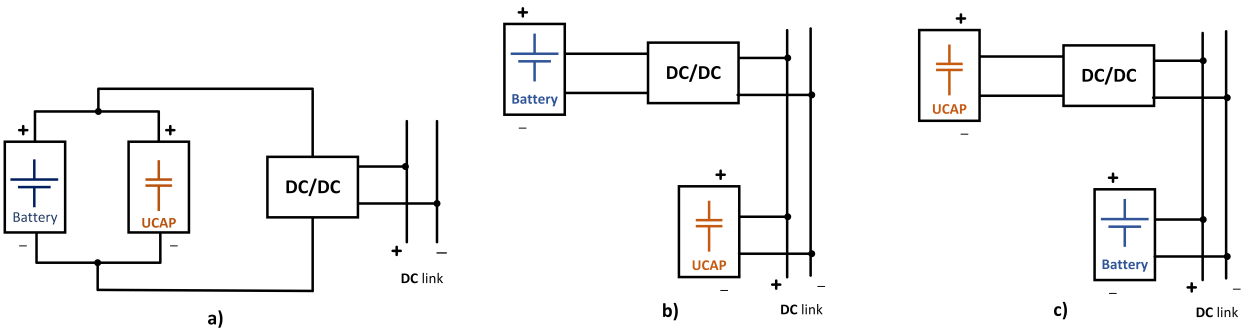

Figure 2. Semi-active HESS topology: (a) pSA, (b) bSA, and (c) cSA.

2.2. Active HESS

The energy storage devices must be decoupled [16] to operate each energy storage in a HESS setup optimally. Active connection of the HESS differs from the passive connections due to the inclusion of converters to decouple the effects of the battery and the UCAP. Active architectures offer the most scalability, stability, control, and operational flexibility; the specific attributes that are favored in a particulat setup depend on the active configuration. The two broad categories of active HESS are semi-active (SA) and full active (FA) sub-topologies, which vary based on the connection of storage devices to DC bus. In both sub-topologies the limitations of the passive connection are corrected using additional DC/DC converters. The SA HESS uses one additional DC/DC converter whereas in the FA HESS the number of DC/DC converters depends on the number of individual energy storage types or individual energy storage devices. The requirement of additional DC-DC converters to decouple the pSA and the cFA topologies adds to increased costs, thermal loss and control logic complexity.

2.3. Semi-active topology

The semi-active topology is composed of only one converter connected to the energy storage systems. The possible configurations are:

- **Parallel Semi-Active (pSA)** (Fig. 2(a)) This configuration is composed of the battery and UCAP connected in parallel to a bi-directional DC-DC converter. This decoupling enables the operating voltage range of the HESS to be independent of the voltage across the load. The DC-DC converter should facilitate the maximum load current and power of the load connected to the HESS. The total load power should be fed as the power command input to the bidirectional DC-DC converter to achieve maximum contribution from the HESS [5].

- **Battery Semi-Active (bSA)** (Fig. 2(b)) This topology decouples the battery from the UCAP using a DC-DC converter. Although this configuration provides a stress free operation for the battery, due to the support from the converter, the UCAP cannot be used to its full potential due to its linear discharge property [17]. The ideal ramping capacity of the UCAP should be exponential, which is not economically practical because it requires a very large UCAP rating.

- **Capacitor Semi-Active (cSA)** (Fig. 2(c)) This configuration enables the decoupling the UCAP from the battery using a bi-directional DC-DC converter and a direct connection of the battery to the DC bus, providing a larger range of voltage response characteristics from the UCAP. However, the battery being directly connected to the DC bus shares a fair proportion of current peaks with increased load demand, introducing stress on the cells and reducing the life-cycle of the battery [18]. The high load current for an instantaneous power delivery elevates the discharge rate and current of the battery [19].

2.4. Full-active topology

The full-active (FA) topology consists of individual converters for both the battery and the UCAP. The FA topology can be broadly classified as parallel full-active (pFA) (Fig. 3(a)) and cascaded full-active (cFA)(Fig. 3(b)). This configuration allows the battery and UCAP to utilize their full range of operating regions by decoupling them individually. An active HESS configuration makes the best use of the available UCAP energy. However, the addition of power electronic

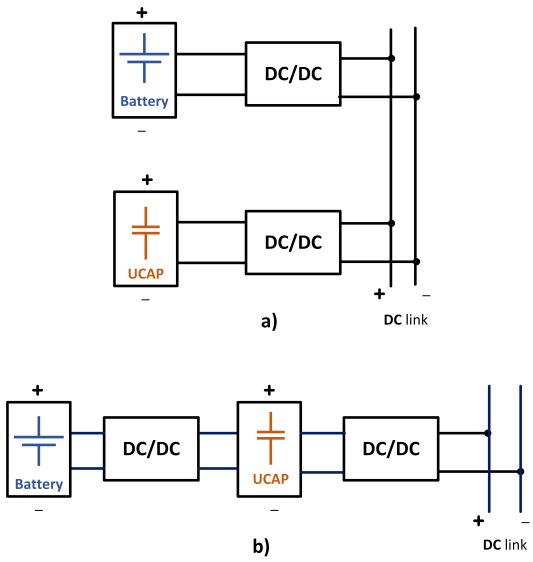

Figure 3. Full-active HESS topology: (a) pFA and (b) cFA.

devices leads to more complexity of operation and higher overall cost [6].

3. Simulation Framework

This section describes the 2-bus test system, hydropower generator-turbine governor model, associated controls, and models for battery and UCAP devices.

3.1. Test System

The 2-bus test system was designed in the MATLAB/Simulink digital platform, using the Simpower Systems / Simscape toolbox [20]. The ROR hydropower plant is considered to be operating in an isolated mode, interfacing with the DC coupled HESS via the dynamic load models (Fig. 4). The hydro generator is equipped with the hydro-turbine governor model and excitation systems. The hydro governor model is based on the permanent droop based PID control driven model of the governor gate opening/closing. The model is derived from [21, 20] where the static gain of the governor is equal to the inverse of the permanent droop R_p in the feedback loop. The PID regulator has a proportional gain K_p, an integral gain K_i, and a derivative gain K_d. The high-frequency gain of the PID is limited by a first-order low-pass filter with time constant T_d(s).

Table 1. System parameters used in simulation

Components	Parameters	Values
Buck/Boost Converter	Switches	MOSFET
	Inductor	1 mH
	Switching Frequency	10 kHz
	DC Bus Voltage	1040 V
	Controller Parameters	K_p = 1.5, K_i = 1
UCAP	Capacitance	9.2 F
	Voltage	1040 V
	Modules	N_s = 8, N_p = 1
	Operating Temperature	25 °C
Battery	Model	Lithium-ion
	Nominal Voltage	264 V (active), 900 V (passive)
	Rated Capacity	660 Ah
	Rated Energy	174.24 kWh
	Response Time	30 s
Generator	Rated Power	20 MVA
	Rated Rms Voltage	13.8 kV
	Reactances	(p.u.)
	X_d, $X_d^{'}$, $X_d^{''}$	1.305, 0.296, 0.252
	X_q, $X_q^{'}$, $X_q^{''}$	0.474, 0.243, 0.180

Components	Specifications
Excitation System	IEEE type 1 voltage regulator combined to an exciter [20]
Governor	Hydraulic turbine combined to a PID governor system [20]

3.2. Droop Control Design

The HESS integrated with ROR hydropower unit uses a power-frequency droop control (Fig. 5). The power required by the HESS is determined by the frequency deviation of the generator due to change in system operations. The difference in the measured frequency versus the frequency reference controlled by a droop gain (K) to generate the required power command for the battery and the UCAP. The droop gain (K) is set to (2×10^5) so that the deviation in frequency sets the power reference command to the HESS. The power reference is subject to a battery power rate limiter (RL) that is kept at 3 kW/s to act as a ramping constraint for the battery. The UCAP power reference is derived from the difference of the total output and the battery constrained output. The time constant for the low-pass filter is set to $T_s = 0.1s$.

3.3. Battery and UCAP Model

We use the UCAP model available from MATLAB/Simulink model [20]. This model is based on the Stern principle and is a combination of the Helmholtz model and Gouy–Chapman model [22]. The UCAP model consists of multiple cells connected in series-parallel combination to achieve the desired current and voltage ratings. Each cell is assumed to

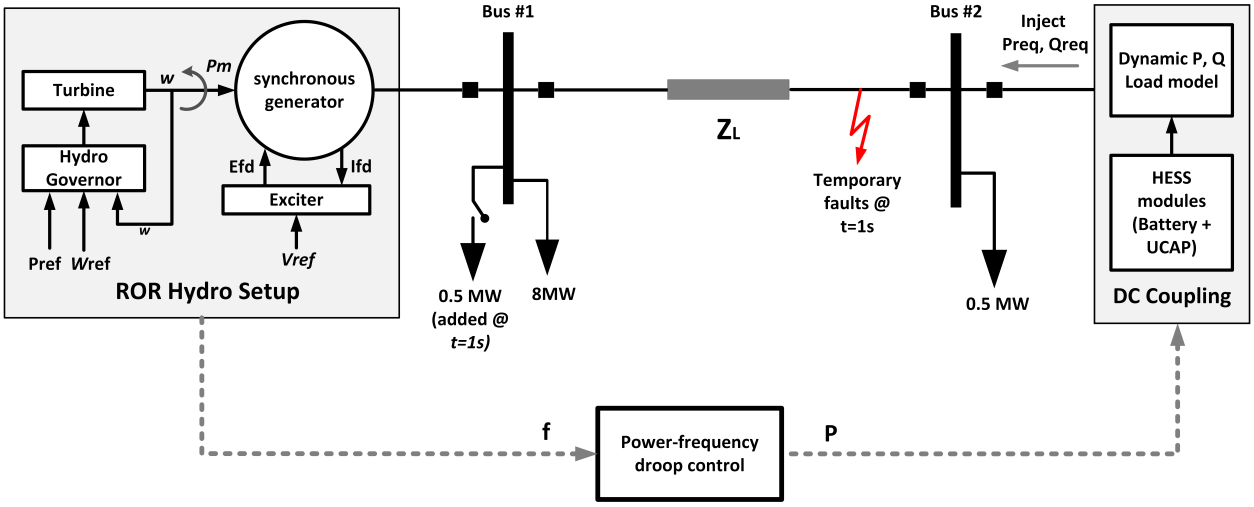

Figure 4. 2-Bus test system.

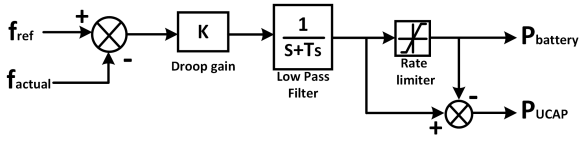

Figure 5. Power-frequency droop control for HESS integration with ROR hydropower.

have a capacitance of C F. The total capacitance C_T of this arrangement of N_P number of parallel cells and N_S number of series cells can be given as

$$C_T = \frac{N_P}{N_s} C \tag{1}$$

Values of these parameters are specified in table 1. Within battery technologies, this paper focuses on lithium-ion chemistries, because this is presently the most commonly deployed type for grid-scale applications [1].

4. Simulation Results

We implemented and compared performance of the six HESS topologies (Passive, pSA, bSA, cSA, pFA, and cFA) for an isolated grid with a hydropower plant. The results of these simulations are first presented based on the performance of each topology and then compared across simulations to asses relative technical performance and corresponding estimates of financial value. Simulation results in the following subsections are displayed in per unit (p.u.) format with the frequency base kept at 60 Hz and the power base kept at 10 kW for better visualization.

4.1. Passive HESS

The passive HESS test system was simulated by connecting the passive HESS topology to the hydro generator model and subjecting it to different conditions like change in loading on the generator bus and temporary faults. In Fig. 6, the system frequency response can be observed for a temporary 3ϕ fault near bus 2.

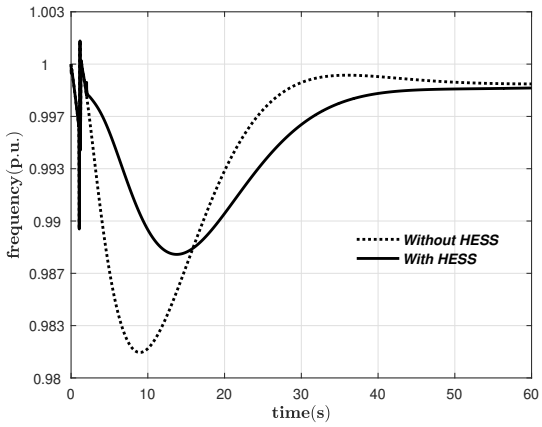

Figure 6. Grid frequency response for the passive HESS subject to a 6-cycle, 3ϕ-fault.

The governor responds to the change in frequency and provides support in reasonable time frame ($\approx$ 30s to steady-state) but the passive HESS provides a much better frequency nadir and rate of change of frequency (RoCoF) (Fig. 6). Another scenario is tested with the passive hybrid, in which a $0.5MW$ change in active loading is carried out at (t=1s) at bus $\#1$ (Fig. 7). The

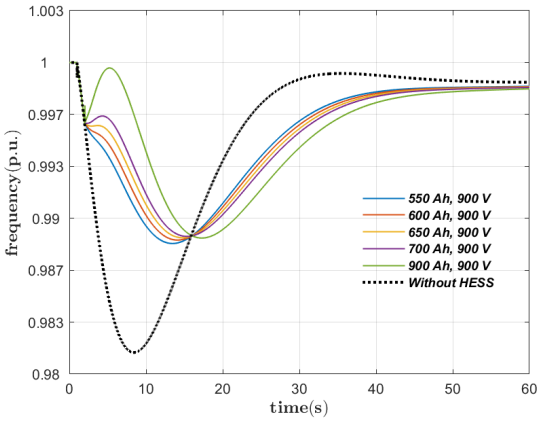

Figure 7. Grid frequency response for the passive HESS subject to a 0.5 MW change in loading, with variation in battery Ah capacity.

capacity rating of the battery have been varied between $550Ah$-$900Ah$ at a fixed voltage output of $900V$ to check the effectiveness of this configuration for different size batteries. The frequency nadir improves with increases in the battery Ah capacity. Thus, increasing performance of the passive hybrid is increases with a larger, and more expensive, battery ratings and the large voltage range of operation. The UCAP, on the other hand, supplies a constant power instead of ramping up, so power rendered by the UCAP in the passive hybrid toplogy is limited.

The power injected from the battery in the passive hyvbrid is much higher than that from UCAP (Fig. 8), leading to faster degradation of the battery [18].

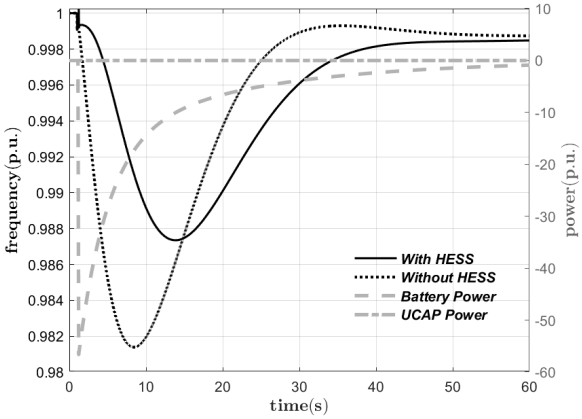

Figure 8. Grid frequency response for the passive HESS subject to a 0.5 MW change in loading.

4.2. Active HESS

The active HESS topologies tested are parallel semi-active (pSA), parallel full-active (pFA), and cascaded full-active (cFA) (Fig. 4). The active HESS topologies are simulated as current injection models using dynamic load components.

During active loading, the pSA leads to improved frequency nadir and faster response than passive HESS. (Fig. 9). The power injected by the battery and the UCAP can also be observed in Fig. 9. The battery and UCAP provides the initial transient power required to improve the drop in instantaneous frequency whereas the UCAP is supporting the battery with a steady discharge rate as time progresses, something that is contradicting with the required behavior of the UCAP, which should be instead providing the ramping support. The UCAP provides an initial power ramp of 1.152 p.u. and reaches steady-state near (t=$20s$) with a stead-injection of 0.016 p.u. for the rest of the time-response. It is evident that the pSA topology although being cost-effective due to the need of only one bi-directional DC-DC converter, suffers a lack of continued power ramping support from the UCAP. With the most of power ramping, the battery would degrade fasetr which is undesirable and not very efficient [18]. Compared to the passive HESS configuration (Fig. 8), the UCAP performs better in case of the pSA configuration (Fig. 9), which is due to the presence of the converter in the latter that decouples its response from that of the battery.

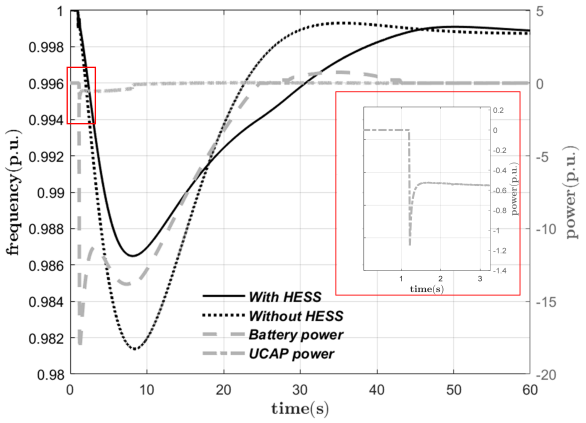

Figure 9. Grid frequency response for the pSA HESS subject to a 0.5 MW change in loading.

The bSA and cSA configurations were also tested for the same conditions but both of them demonstrated unacceptable frequency drops and are therefore not included here. The DC-DC converter must be designed

to accept short bursts of high-power peaks and the high voltage swings in these configurations, which in turn affects the cost of the system [23]. There might be a higher chance of failure of the DC-DC converters in these setups, and in that case the power burden needs to be shared completely by the UCAP, making it prone to faster discharge rates.

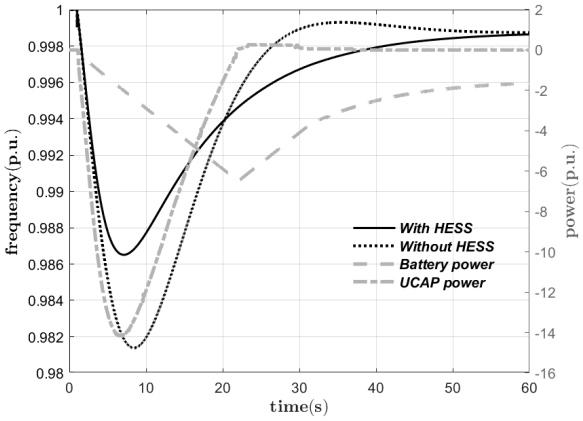

Figure 10. Grid frequency response for the pFA HESS subject to a 0.5 MW change in loading.

During a loading condition on the grid, both the full-active configurations utilize the UCAP's potential to its fullest by supplying the instantaneous power injection to improve the frequency response (Figs. 10 and 11).

The battery injects power at a relatively slower rate in these configurations, leading to enhanced battery life and performance, as well as contributing to a better frequency nadir over the operation period.

Comparing initial ramp rates for the active HESS configurations, the pFA and cFA provide similar initial ramp rates with respect to the UCAP and battery (Table 2). This is mostly due to their independent operating range decoupled by the bidirectional DC-DC converters. In case of the pSA, both the battery and UCAP contribute to the initial ramp response, but the battery seems to be contributing more compared to the UCAP. This reinforces the fact that the operating voltage window in the pSA topology is in general determined by the battery storage, which limits the usable capacity of the UCAP.

During a self-clearing temporary 3ϕ-fault when connected via the full-active HESS modules, it can be observed that the full-active configurations have similar frequency nadir but the cFA configuration has a better return to steady-state (Fig. 12). The main objective of this test was to validate the effectiveness of the HESS modules in case of major contingencies like temporary

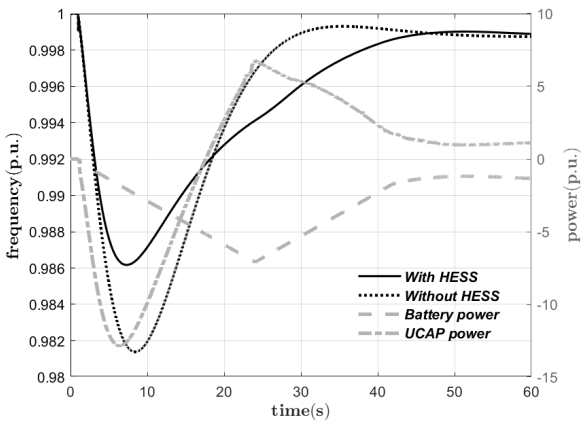

Figure 11. cFA HESS frequency nadir during a 0.5 MW change in loading.

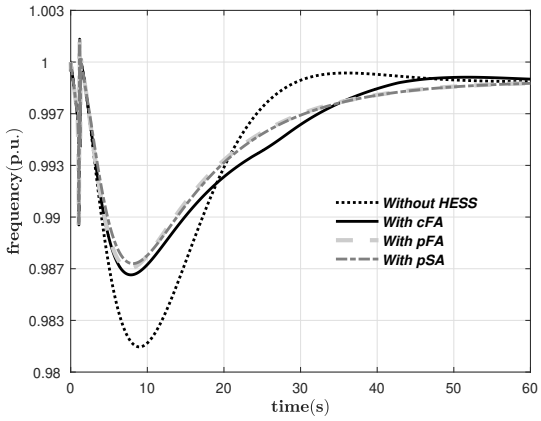

Figure 12. FA HESS frequency nadir during a 3ϕ,6-cycle fault on line connecting bus$\#1$ and $\#2$ in Fig. 4.

fault condition on the grid.

Table 2. Initial ramp rates for active HESS

HESS Topology	Ramp Rates [kW/min]	
	UCAP	Battery
pSA	7854	230×10^3
pFA	1512	183
cFA	1499	186

5. Concluding Remarks

We provide an overview of the passive and active hybridization of electric energy storage systems and integrate them with an ROR hydropower plant in a 2-bus demonstration system to assess grid scale response.

First, the existing literature in hybrid module in the electric vehicle domain are investigated and ideas are leveraged to accommodate similar hybrid topologies in grid applications integrated with an ROR hydropower plant. This integration enhances the capability of the ROR hydropower plant to inject or absorb power as required to provide specific grid services. Here, we investigate the ability to provide frequency response in an islanded grid setting. The same capability can also be used to provide frequency regulation in an ancillary services market.

The simulations compare the HESS topologies' response to grid scale contingencies such as active loading on the generator bus and temporary faults. For the proposed hybridization, the battery and the UCAP are used as a backup source which provides the power required, when the power given by hydro generator is not sufficient to supply the load. The passive and semi-active HESS topologies shows significant improvements in the frequency response during both events, but decrease battery life due to over-stressing and requires a significantly larger (and more expensive) battery capacity. The DC bus voltage is uncontrollable in the case of the parallel topology given the absence of decoupling between the battery and UCAP. The full-active HESS topology provides the best frequency improvement performance and retains the operational limits of the energy devices by decoupling them using individual DC-DC converters, either in series or parallel combinations.

Large hydropower plants have long been critical black start resources, but research led by Idaho National Laboratory is presently demonstrating that low-head ROR hydropower plants integrated with energy storage, such as UCAP or HESS, can also provide black start services [24]. This would improve the ability of smaller hydropower plants tied to the distribution system to black start an islanded portion of the grid if the transmission system goes offline. This points to the ability of integrated HESS and generation resources to provide a range of services, increasing the value of the investment. Detailed investigations will be undertaken in future work to examine other aspects of the proposed topologies, including comparison to an AC coupled battery and UCAP hybrid energy storage system and its cost-benefit analysis for providing fast frequency response (isolated or combined with inertial response in an integrated system) [25] and IEEE 1547-2018 mandated reactive power support [26] to provide additional flexibility and independent operational capabilities.

6. Acknowledgement

This manuscript has been authored by Battelle Energy Alliance, LLC under Contract No. DE-AC07-05ID14517 with the U.S. Department of Energy. Work supported through the U.S. Department of Energy Water Power Technology Office HydroWIRES Initiative.

References

[1] K. Mongird, V. Viswanathan, P. Balducci, J. Alam, V. Fotedar, V. Koritarov, and B. Hadjerioua, "Energy storage technology and cost characterization report," tech. rep., July 2019.

[2] R. Hemmati, "Optimal cogeneration and scheduling of hybrid hydro-thermal-wind-solar system incorporating energy storage systems," Journal of Renewable and Sustainable Energy, vol. 10, no. 1, p. 014102, 2018.

[3] Electric Power Research Institute, "Flexible operation of hydropower plants," May 2017.

[4] A. Khaligh and Zhihao Li, "Battery, Ultracapacitor, Fuel Cell, and Hybrid Energy Storage Systems for Electric, Hybrid Electric, Fuel Cell, and Plug-In Hybrid Electric Vehicles: State of the Art," IEEE Transactions on Vehicular Technology, vol. 59, pp. 2806–2814, July 2010.

[5] A. Kuperman and I. Aharon, "Battery–ultracapacitor hybrids for pulsed current loads: A review," Renewable and Sustainable Energy Reviews, vol. 15, no. 2, pp. 981 – 992, 2011.

[6] J. Shen, S. Dusmez, and A. Khaligh, "Optimization of sizing and battery cycle life in battery/ultracapacitor hybrid energy storage systems for electric vehicle applications," IEEE Transactions on Industrial Informatics, vol. 10, pp. 2112–2121, Nov 2014.

[7] D. B. W. Abeywardana, B. Hredzak, V. G. Agelidis, and G. D. Demetriades, "Supercapacitor sizing method for energy-controlled filter-based hybrid energy storage systems," IEEE Transactions on Power Electronics, vol. 32, pp. 1626–1637, Feb 2017.

[8] "Duke energy to put new battery and ultracapacitor system to the test in N.C.," March 2016.

[9] T. Zimmermann, P. Keil, M. Hofmann, M. F. Horsche, S. Pichlmaier, and A. Jossen, "Review of system topologies for hybrid electrical energy storage systems," Journal of Energy Storage, vol. 8, pp. 78 – 90, 2016.

[10] K. Engeland, M. Borga, J.-D. Creutin, B. François, M.-H. Ramos, and J.-P. Vidal, "Space-time variability of climate variables and intermittent renewable electricity production – a review," Renewable and Sustainable Energy Reviews, vol. 79, pp. 600 – 617, 2017.

[11] US Department of Energy, "Hydropower Vision - A New Chapter for America's 1^{st} Renewable Electricity Source," 2015.

[12] T. Wang, "Battery assisted conventional generator in pjm frequency regulation market.," in 2019 IEEE PES General Meeting, pp. 1–5, Aug 2019.

[13] S. Pay and Y. Baghzouz, "Effectiveness of battery-supercapacitor combination in electric vehicles," in 2003 IEEE Bologna Power Tech Conference Proceedings,, vol. 3, pp. 6 pp. Vol.3–, 2003.

[14] R. A. Dougal, S. Liu, and R. E. White, "Power and life extension of battery-ultracapacitor hybrids," IEEE Transactions on Components and Packaging Technologies, vol. 25, no. 1, pp. 120–131, 2002.

[15] Hybrid Energy Storage System for Hybrid and Electric Vehicles: Review and a New Control Strategy, vol. Volume 4: Energy Systems Analysis, Thermodynamics and Sustainability; Combustion Science and Engineering; Nanoengineering for Energy, Parts A and B of ASME International Mechanical Engineering Congress and Exposition, 11 2011.

[16] S. F. Tie and C. W. Tan, "A review of energy sources and energy management system in electric vehicles," Renewable and Sustainable Energy Reviews, vol. 20, pp. 82 – 102, 2013.

[17] L. Gao, R. A. Dougal, and S. Liu, "Active power sharing in hybrid battery/capacitor power sources," in Eighteenth Annual IEEE Applied Power Electronics Conference and Exposition, 2003. APEC '03., vol. 1, pp. 497–503 vol.1, 2003.

[18] B. Xu, A. Oudalov, A. Ulbig, G. Andersson, and D. S. Kirschen, "Modeling of lithium-ion battery degradation for cell life assessment," IEEE Transactions on Smart Grid, vol. 9, no. 2, pp. 1131–1140, 2018.

[19] A. Etxeberria, I. Vechiu, H. Camblong, and J.-M. Vinassa, "Comparison of three topologies and controls of a hybrid energy storage system for microgrids," 2012.

[20] MATLAB, 9.8.0.1323502 (R2020a). Natick, Massachusetts: The MathWorks Inc., 2020.

[21] "Hydraulic turbine and turbine control models for system dynamic studies," IEEE Transactions on Power Systems, vol. 7, no. 1, pp. 167–179, 1992.

[22] K. B. Oldham, "A gouy–chapman–stern model of the double layer at a (metal)/(ionic liquid) interface," Journal of Electroanalytical Chemistry, vol. 613, no. 2, pp. 131 – 138, 2008.

[23] A. Ostadi, M. Kazerani, and S. Chen, "Hybrid energy storage system (hess) in vehicular applications: A review on interfacing battery and ultra-capacitor units," in 2013 IEEE Transportation Electrification Conference and Expo (ITEC), pp. 1–7, 2013.

[24] "Integrated Hydropower Storage Systems (INL)," 2016.

[25] NERC Inverter-Based Resource Performance Task Force, "Fast frequency response concepts and bulk power system reliability needs," tech. rep., March 2020.

[26] IEEE Standards Association, "1547-2018 - IEEE Standard for Interconnection and Interoperability of Distributed Energy Resources with Associated Electric Power Systems Interfaces," April 2018.